FINITE DIFFERENCE MODELING OF AUTOGENEOUS TIG WELD POOL PROFILES

نمذجة برك لحام التيج بطريقة الفروق المحددة

G. A. NASSEF*, M. M. ABDELRAHMAN** AND A. M. AL- BAHI***
* Assoc. Prof., Production Engrg. Department, Faculty of Engineering Alexandria University, Egypt
** Prof., Aeron. Engineering Department, Faculty of Engineering Cairo University, Egypt
*** Assoc. Prof., Aeron. Engrg. Department, Faculty of Engineering, King Abdulaziz university, Saudi Arabia.

ملخص: تم في هذا البحث توليد برك لحام التيج معمليا في عينات اسطوانية من الصلب الكربوني. و تناولت التجارب ظروف مختلفة من تيار القوس؛ وقطر فوهة الأرجون؛ وزمن تعرض المعدن للقوس. وقد تم قياس كل من قطر و عمق برك اللحام المتولدة؛ و من ثم تحديد أشكالها. كما تضمن البحث استخدام نموذج رياضي لمعادلات انتقال الحرارة و معادلات الحركة في مانع اللحام لاستنتاج شكل بركة اللحام رقميا. وقد تم مقارنة النموذج النظري بالنتائج المعملية لاستنتاج القيم المثلى لكل من معامل التوزيع الحراري ؛ و كفاءة القوس الكهربي. وقد حقق النموذج الرياضي تطابقا أفضل مع النتائج المعملية مقارنة بالنتائج السابقة؛ وذلك في حدود المدى المدروس لمتغيرات اللحام.

ABSTRACT

In this paper experimental weld pools has been created in axisymetric specimens of low carbon steel by autogeneous gas tungsten arc (GTA). Different conditions of arc current, nozzle size and arc time have been investigated. The weld pool profile has been measured and plotted in each case. A numerical heat transfer model that takes into account fluid flow in the weld pool was employed to simulate the development of GTA welding process. The model has been tested against the experimental results to deduce the optimum values of arc efficiency and heat distribution parameter. The model provides far better fit to the experimental results for the whole investigated range of parameters as compared to previous models. The degree of accuracy of the model is not affected by the arc time within the investigated range. The results have been discussed and interpreted.

INTRODUCTION

A growing recognition of significant fluid flow during fusion welding has been manifested in previous investigations. Various mathematical models have been formulated to describe heat and fluid flow in several welding processes including Gas Tungsten Arc(GTA) [1], Gas Metal Arc (GMA) [2,3], Electron Beam (EB) [4], spot [5] (SW) and Laser Beam (LB) [6] welding. The accuracy of the obtained numerical results depends upon the selection of such parameters as arc efficiency and heat distribution parameters. In a recent work [3], an attempt has been devoted to study the influence of these parameters on the weld pool profiles in GTAW and GMAW. It has been concluded that the heat distribution parameter has a considerable influence on the depth of the weld pool. The width of the weld pool was found to be more sensitive to variations of arc efficiency. Hitherto, the choice of these model parameters has been based on mere assumptions.

Accepted 4 Nov. 1996

in the present investigation, a transient heat transfer model has been used with an experimental program to model GTA weld pools. Experimental results are used with the previously developed numerical model to deduce most accurate values of model parameters. The selection of these values is based on testing the model against experimental weld pool profiles under different welding conditions.

EXPERIMENTAL PROCEDURE

Weld Pool Generation

Gas tungsten arc has been used to create weld pools at the center of cross section : along the axis of identical mild steel cylinders of 45 mm diameter X 40 mm height. A fixture is specially designed to hold the specimen (axis in vertical position). The head of gas tungsten arc (GT.) has been used to develop a molten pool, during a predetermined arc exposure time, at the center of one face of the cylinders. The arc current has been varied to include the values 100, 150, and 200 amp. The investigated arc exposure times are 3, 5, 8, and 12 Sec. Two nozzle sizes of 9 and 12 mm diameter has been used.

The specimens,after exposure to the GTA were instantly immersed in water. The specimens were then sectioned longitudinally and then polished and etched to reveal the weld pool boundary. Two traversing perpendicular micrometers have been used to obtain the coordinates of

the contour points. Special precautions were taken to insure measurement along the diameter of the pool for width measurements and maximum value was also taken for weld pool depth.

MATHEMATICAL MODEL

Fig. 1 shows a schematic representation of the arc weld pool interaction in gas tungsten arc. The arc is struck between a tungsten non consumable electrode and a molten metal pool formed due to the heat flux falling on the metal surface. The problem is defined as a spatially and time dependent heat received by the metal block at the free surface as well as the unsteady growth of the weld pool.

Following previous investigations the proposed model is based on mathematical representation under the following assumptions:

- Both heat transfer and fluid flow inside the molten pool are adequately described by an axisymetric constant density model using the vorticity stream function formulation
- In the present case low current welding is assumed, therefore the turbulent nature of flow can be neglected.
- The fluid flow field represented in the weld pool is driven by a combination of buoyancy, surface tension, and electromagnetic forces.
- To avoid the complexity of energy loss that occur from arc to the metal , an efficiency η is used to quantify the energy made available by the arc to the metal surface.
- The power distribution of the heat source is considered as Gaussian profile.

The effect of vaporization on convection and the heat lost from the surfaces in the form of radiation are neglected.

Based on the above assumptions the governing equations take the following form:

$$\frac{\partial \omega}{\partial t}+U\frac{\partial \omega}{\partial z}+Vr\frac{\partial(\omega/r)}{\partial r}=\upsilon\left[\frac{\partial^2\omega}{\partial r^2}+\frac{\partial}{\partial r}(\frac{\omega}{r})+\frac{\partial^2\omega}{\partial z^2}\right]+g\beta(\frac{\partial T}{\partial r})+\nabla\wedge(J\wedge B) \qquad (1)$$

$$\omega+\frac{\partial}{\partial r}(\frac{1}{r}\frac{\partial \psi}{\partial r})+\frac{\partial}{\partial z}(\frac{1}{r}\frac{\partial \psi}{\partial z})=0 \qquad (2)$$

$$\frac{\partial T}{\partial t}+U\frac{\partial T}{\partial z}+V\frac{\partial T}{\partial r}=\frac{1}{\rho C_p}=\left[\frac{1}{r}\frac{\partial}{\partial r}(kr\frac{\partial T}{\partial r})+\frac{\partial}{\partial z}(k\frac{\partial T}{\partial z})+\Delta H\right] \qquad (3)$$

with

$$U=\frac{1}{r}\frac{\partial \psi}{\partial r} \qquad \text{and} \qquad V=\frac{1}{r}\frac{\partial \psi}{\partial z} \qquad (4)$$

Where ψ is the stream function, ω is the vorticity, U and V denote the velocity components in the axial Z and radial r directions respectively. ρ, p and T are the thermodynamic properties (density, pressure, and temperature) of the molten pool . ν, C_p and k are the kinematics velocity, specific heat and thermal conductivity respectively. ΔH is the energy exchange between the spray droplets and molten pool, for the case of GMAW, while for GTAW, $\Delta H=0$. The two last terms in equation (1) represent the buoyancy and electromagnetic forces respectively.
The detailed equations and the data used for the numerical computations are given in details in the author s previous work [3].

The above equations are used to calculate the temperature distribution and the weld pool configuration of the workpiece, with the help of the following boundary conditions:

1. The heat transfer between the surface of the workpiece and the arc is described by a Gaussian distribution.

2. The heat transfer at the bottom of the workpiece is calculated by equating the conduction heat flux with heat flux due to convection from the metal.

3. The no slip conditions are imposed along the solid liquid interface.

4. At the surface of the pool, the surface tension variations with temperature must be balanced by fluid shear. Therefore, the shear stress at the surface is equated to the gradient of surface tension.

5. On the axis of symmetry , i.e. at $r = 0$, the conditions of symmetry are applied.

A computational model is developed to investigate the fluid flow and the heat transfer during the welding process. The above governing equations are descrtuzed using the finite difference technique with a non-uniform mesh grid. The equations are then integrated numerically using an implicit ADI method.

RESULTS AND DISCUSSION

A recent model by the same authors [3] predicted a weld pool of about the same depth but of fairly larger width than the experimental one. It has been also stated that the accuracy of numerical weld pool profile depends on the selected values of the heat distribution parameter r_b and the arc efficiency parameter (η).

Chrisensen et al. [7] reported values between 0.66 and 0.69 for arc efficiency (η) for GMAW of mild steel. Essers et al. [8] allocate a value of 0.71±0.03 to the same parameter. However little is known about the useful range of r_b. The present finite difference model is used here-in to correlate the weld pool depth to the parameter r_b at different values of η, welding current and arc time. These numerical results are shown in Fig. 2. As previously concluded, the figures show that the depth of the weld pool increases as the value of r_b increases.

These figures are used to predict the optimum values of η and r_b for the present experimentation in the following procedure:

Using figure 2, three values of the parameter r_b is obtained for a given experiment at certain arc time, nozzle size and arc current by measuring the corresponding experimental depth of the weld pool and the value is plotted as a horizontal straight line on Fig. 2, to find r_b for the three different values of η.

For the two different nozzles the values obtained in step 1 are plotted to obtain correlation of arc parameters for different nozzle diameter, arc time and arc current. This correlation are shown in Fig. 3.

The arc efficiency parameter η is taken to be 0.70, for the two nozzles, and accordingly the values of r_b for each current and nozzle diameter can be obtained from figs 3 as shown in table (1)

Table 1 Heat distribution parameter as deduced from correlation

Arc current (amp)	Nozzle size (mm)	Heat distribution parameter (rb)
100	9	4.82×10^{-3}
	12	3.50×10^{-3}
150	9	5.30×10^{-3}
	12	4.95×10^{-3}
200	9	5.85×10^{-3}
	12	5.63×10^{-3}

In the range of experimental investigation it is important to notice from Figs.3 that the values of η and r_b do not depend practically on the arc time and therefore, these parameters are considered constant during the melting process for any arc time.

The developed model is used to predict the experimental weld pool using the revised values of r_b. The theoretical profiles are compared to the experimental ones as shown in Figs. 4. It is shown from the comparison that the model provides better fit to the experimental results, for all the investigated range of parameters as compared to previous investigations [2&3]. The deviations between numerical and experimental weld profiles in the width direction are negligible as compared to the previous study [3]. It is also important to note that the degree of accuracy of the model is not affected by the arc time from the range from 3 to 12 sec.

The influence of nozzle diameter on the resulting pool has been also studied. Fig. 5 shows the profile of the weld pool at different conditions of nozzle size and arc current. The figure elucidates that at low current the nozzle diameter has a considerable influence on both weld pool width and depth. Large nozzle provided wider and deeper weld pool. Meanwhile, the effect of nozzle size becomes negligible at high current. This is alternatively shown in Fig. 6. This figure indicates that at high current the influence of nozzle size on both the depth and the width is negligible, whereas at low current considerable effect is manifested specially on the depth of the weld pool. A narrow nozzle is associated with a considerable drop of melting rate as the current is decreased beyond a certain limit(see Fig. 7). It seems that the melting efficiency in the case of narrow nozzle drops sharply at low current. Probably high fraction of the arc heat is dissipated to the nozzle walls as compared to the case of higher current and/ or wider nozzle.

The model has been used to plot the the stream function and the velocity contours of the weld pools at an arc time of 12 sec. Figs. 8&9 show these results for the two nozzles under investigation at arc current of 100 and 200 amp. The small nozzle is associated with a smaller weld pool and lower fluid flow velocity. The velocity field is obviously time dependent and is affected by the intensity of the arc current. A recirculation flow zone in the weld pool is shown in fig. 8 in the counter-clockwise direction The flow moves downward near the electrode axis and upward near the cooler solid liquid interface. The scale length of this circulation zone depends on the nozzle diameter specially at low current. Similar conclusion are drawn for the flow velocities from Fig. 9 where the effect of nozzle diameter is more pronounced at low current. At 100 amp. arc current maximum velocity of 15.7 mm/sec and 55.5 mm/sec are obtained for 9 mm and 12 mm nozzle diameter respectively. At 200 amp. the maximum velocities reach 80.1 and 82.4 mm/sec for the small and large nozzle respectively.

CONCLUSION

A transient heat transfer model that takes into account fluid flow in the weld pool was employed to numerically simulate the development of GTA weld pools. The model has been tested against experimental results covering ranges of welding current, arc time and nozzle size. The optimum values of arc efficiency and heat distribution parameter has been deduced. The following conclusions can be drawn:

1. By choosing the appropriate values of heat distribution parameter the model provides far better fit to the experimental results for the whole investigated range of parameters as compared to previous models.

2. The effect of arc efficiency is not significant if the heat distribution parameter is correctly selected accordingly. At low welding current the nozzle size has a considerable effect on weld pool. Narrow nozzle yielded a narrow but shallow weld pool.

3. At high current, both the experimental and analytical results showed negligible influence of nozzle size on the weld pool geometry.

REFERENCES

1. Heipel, C. R., and Roper, J. R., (1982), "Mechanism for Minor Affecting GTA Fusion Zone Geometry"; Weld. J., Vol. 61(4), pp. 97s-102s.

2. Tsao, K. C., and Wu, C. S., (1988), "Fluid Flow and Heat Transfer in GMA Weld Pools"; Weld. J., Vol. 67(3), pp. 70s-75s.

3. Al-Bahi, A. M., and Abdelrahman, M. M., (1992), "Heat Transfer and Fluid Flow in GTA and GMA Weld Pools"; 4th International Conference of Fluid Mechanics, Alexandria Egypt.

4. Wei, P. S., and Giedt, H. D., (1985), "Surface Tension Gradient Driven Flow Around an Electron Beam Weld Cavity"; Weld. J., Vol. 64A, pp. 251s-259s.

5. Orper, G. M., and Szekely, J., (1987), "A comprehensive Representation of Transient Weld Pool Development in Spot Welding Operations"; Metallurgical. Trans. , Vol. 18A, pp. 1325-1332.

6. Davis, M., Kapadia, P., and Dowden, J., (1986), "Modeling The Fluid Flow in Laser Beam Welding"; Weld. J., Vol. 65(7), pp. 167s-174s.

7. Christensen, N., Davis, V. de L., and Gjermundsen, K., (1965), "Distribution of Temperature in Arc Welding"; British Welding Journal, Vol. 12(2), pp. 54-75.

8. Tekriwal, P., and Mazumder, J., (1988), "Finite Element Analysis of Three dimensional Transient Heat Transfer in GMA Welding"; Weld. J., Vol. 67(7), pp. 150s-156s.

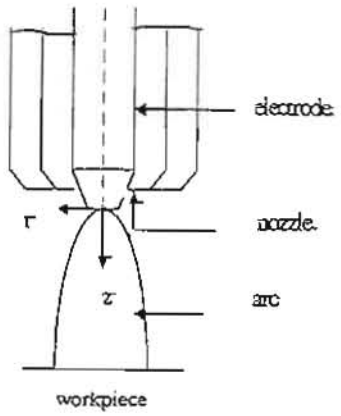

Fig. 1 Schematic of the gas tungsten arc

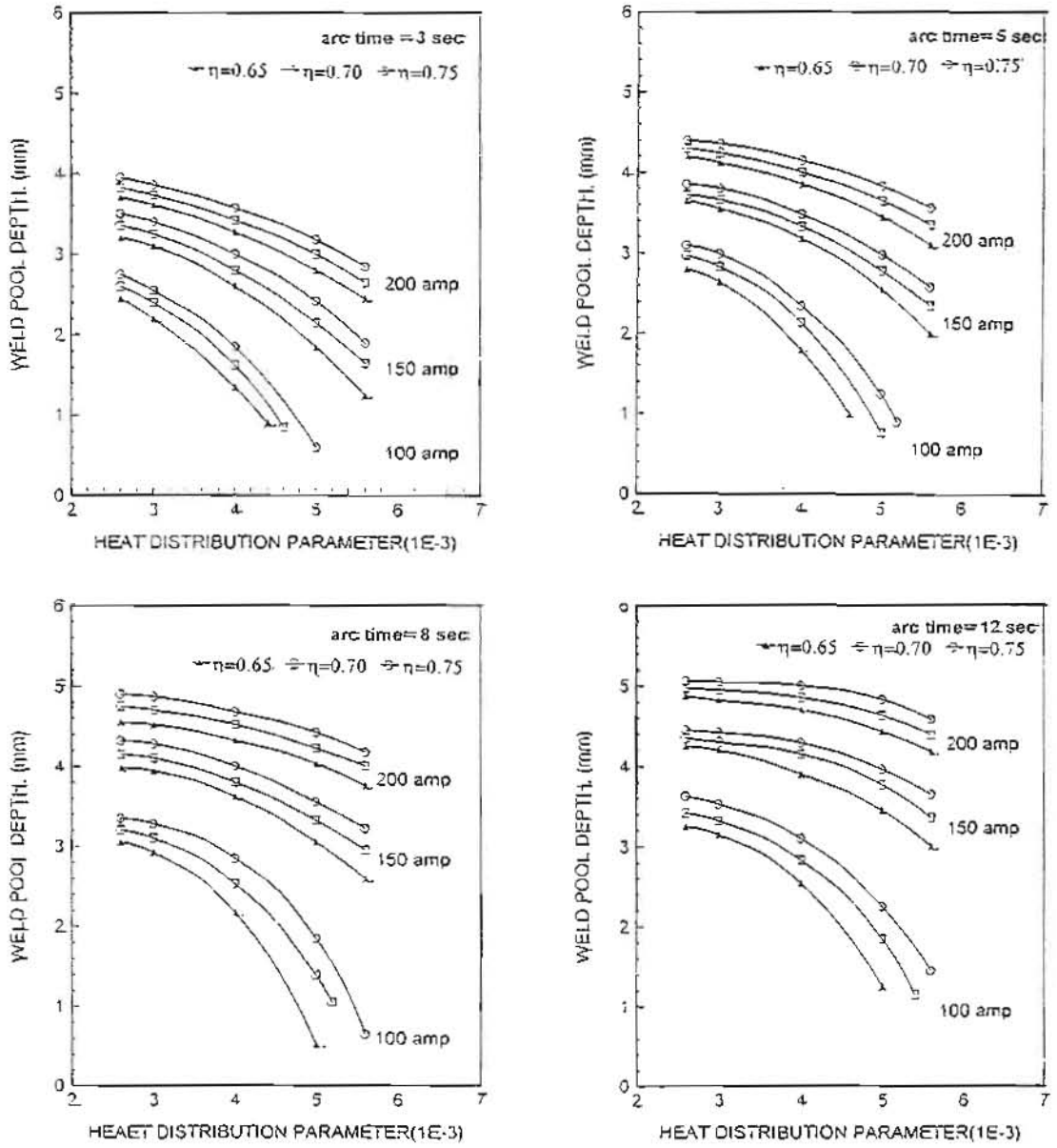

Fig. 2 Influence of both arc efficiency and heat distribution parameters on weld pool depth

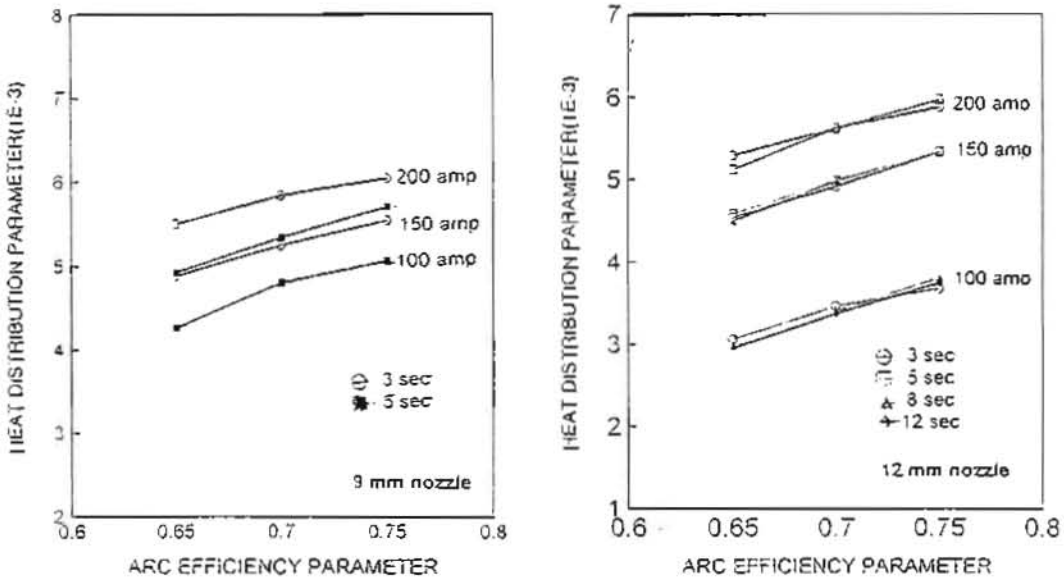

Fig. 3 Heat distribution parameter and arc efficiency as deduced from the model for different arc condition

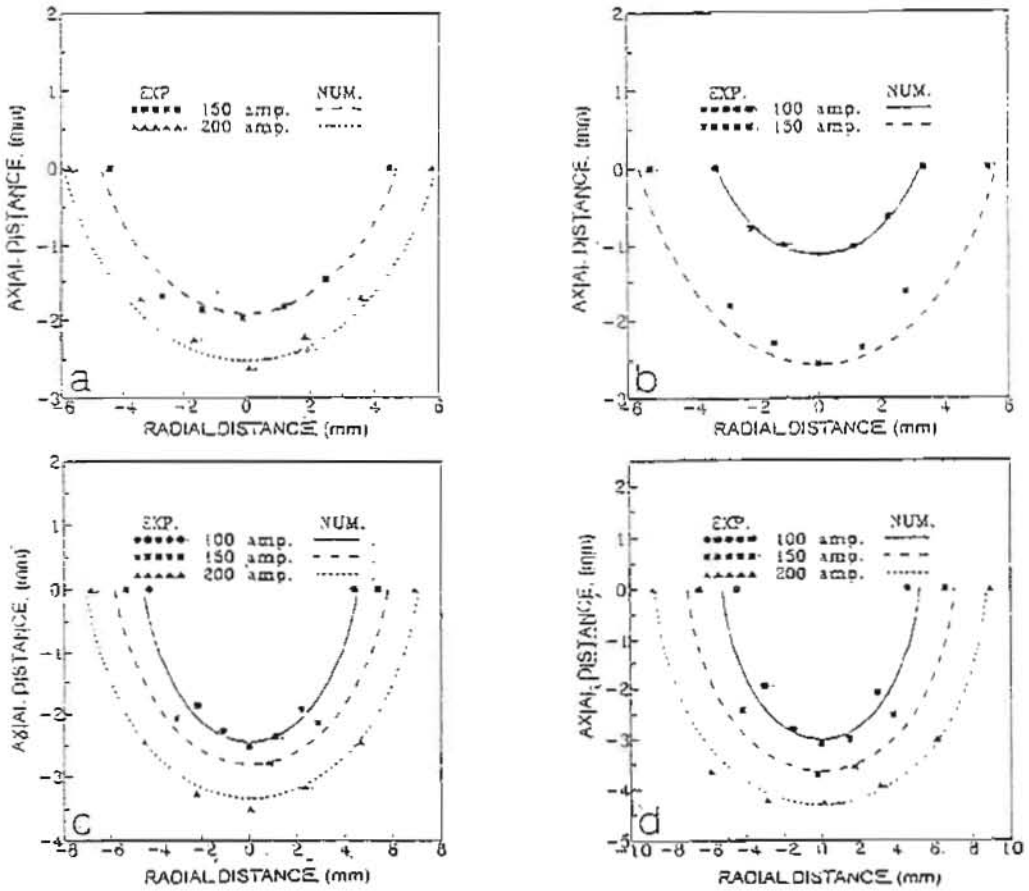

Fig. 4 Experimental weld pool profiles as compared to predicted ones for different arc time, arc current and nozzle size

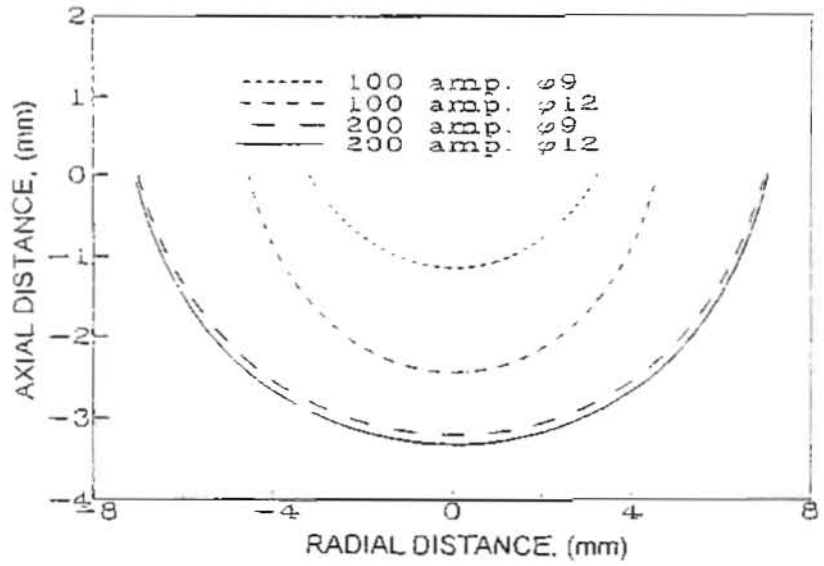

Fig. 5 Predicted weld pool profile after 5 sec for different nozzles and arc current

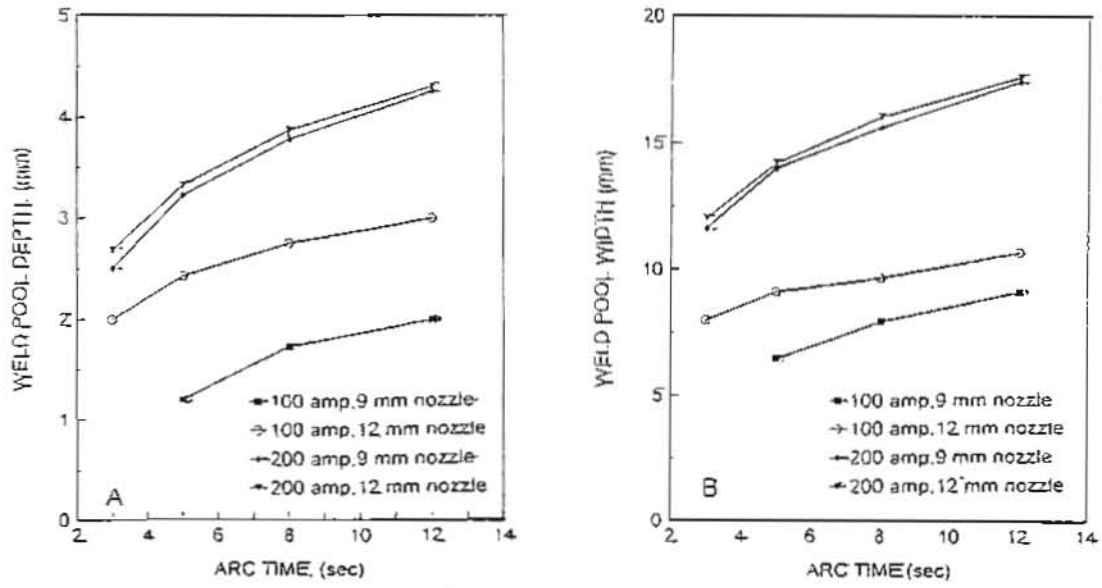

Fig. 6 Evolution of weld pool dimensions with arc time

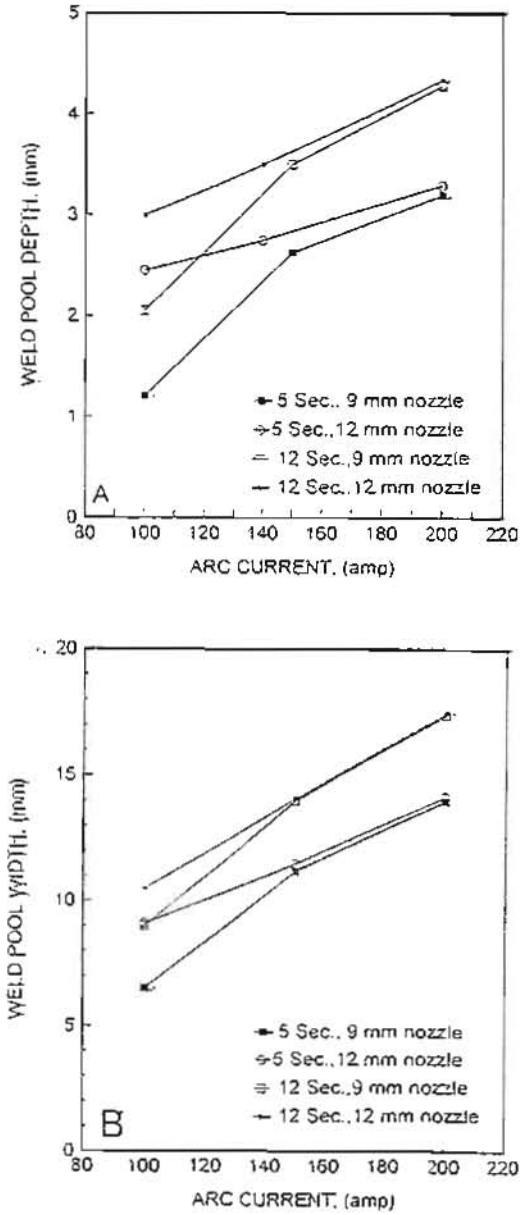

Fig. 7 Effect of arc current on weld pool dimensions

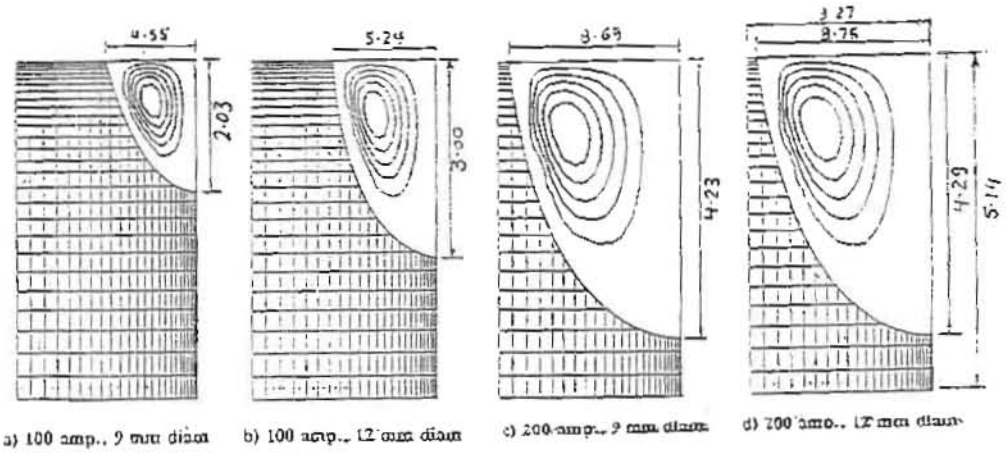

a) 100 amp., 9 mm diam b) 100 amp., 12 mm diam c) 200 amp., 9 mm diam d) 200 amp., 12 mm diam

Fig. 8 Flow pattern of molten metal in the weld pool after 12 sec arc time

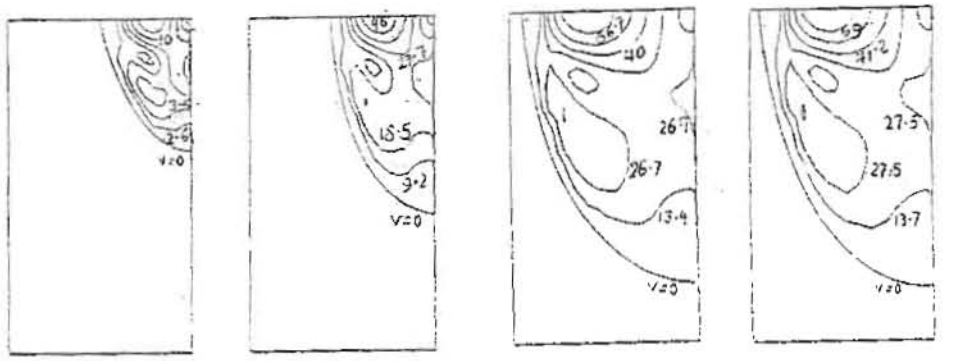

a) 100 amp., 9 mm diam b) 100 amp., 12 mm diam c) 200 amp., 9 mm diam d) 200 amp., 12 mm diam

Fig.9 Velocity contours in weld pool after 12 sec arc time